Advances in Water Resources 74 (2014) 102–115

Contents lists available at ScienceDirect

Advances in Water Resources

journal homepage: www.elsevier.com/locate/advwatres

Analytical solution for enhanced recharge around a bedrock exposure caused by deep-aquifer dewatering through a variable thickness aquitard

Mazda Kompanizare [a,b,*], Jonathan S. Price [a]

[a] Department of Geography and Environmental Management, University of Waterloo, 200 University Ave. West, Waterloo, ON N2L 3G1, Canada
[b] Department of Desert Regions Management, Shiraz University, Shiraz, Iran

ARTICLE INFO

Article history:
Received 4 March 2014
Received in revised form 1 August 2014
Accepted 7 August 2014
Available online 19 August 2014

Keywords:
Mine dewatering
Perched aquifer
Peat
Percolation loss
Steady state
Radially symmetric

ABSTRACT

In this study an analytical solution was developed to predict steady radially-symmetric percolation rates from an aquifer underlain by a variable thickness aquitard. The solutions consider an aquitard with constant thickness and with radial-symmetrically increasing thickness outward from the center. The solution was used to predict the percolation rate from a peat layer around a bedrock outcrop in the James Bay Lowland near the De Beers Victor diamond mine. In this case the marine sediment layer limited the direct connection between the peat layer and the bedrock as an aquitard. Our zero order solution with constant marine sediment thickness showed the best fit to the steady state water level data of June 2012. It was found that the enhanced recharge around bioherms (i.e., at rates greater than the regional average of 0.7 mm/day) will only occur in marine sediments less than 4.3 m thick, for extreme depressurization of 30 m.

1. Introduction

In low-gradient systems, such as coastal plains, perturbations in the groundwater flow-field may be caused by discontinuities in the aquifer structure or by water withdrawals; the system response is closely tied to the vertical structure of its aquifers and aquitards [1–3]. A systematic change in sediment thickness may arise, for example in a depositional marine environment where there are cone-shaped bedrock extrusions. An analytical model of this setting can be used to test its sensitivity to hydraulic conductivity and boundary fluxes, hence potential responses to external stressors such a water withdrawal.

Flow towards a water-sink in a surface aquifer underlain by a layer of low-permeability sediments generates a radial flow towards the sink. Where the aquitard is leaky, there may also be a flow exchange between the perched surface aquifer and an underlying deep aquifer. There are several studies of flow in leaky aquifers solved through analytical [4–11], semi-analytical [12–16] and numerical [17,18] methods. In most of these solutions the aquitard is located above the main aquifer and recharges it. However, a less common situation arises when the aquitard is located at the bottom of the surficial perched aquifer, and controls water discharge from it. As stated by Yeh and Chang [19] in some of these studies the flow in the aquifer is significantly influenced by the drawdown or flow in the adjacent aquitard [6–8,14,15,17]. In these studies the hydraulic conductivity of the aquitard is significantly smaller than that of the aquifer, and so assumes horizontal flow in the aquifer and vertical flow in the aquitard [6–10,17]. In some of these studies the solutions were conducted for two aquifers and an intervening aquitard [13,16,20] but in all of them the aquifer and aquitard thicknesses were constant.

Given the difficulty and expense of empirical studies, the sensitivity of percolation rate to hydraulic head, variations in sediment thickness and permeability are difficult to characterize directly, but can be evaluated using a modeling approach, which is the focus of this paper. In this study the contribution of a bedrock exposure to the enhanced percolation of water from a surficial aquifer, through an aquitard to an underlying depressurized aquifer was conceptualized and evaluated by developing an analytical solution. The solution was conducted for steady and saturated radially symmetric flow in a surficial perched aquifer around a leaky window (bedrock exposure), by considering the pattern of aquitard thickness changes and the head in different layers. In these solutions the first priority was calculation of the percolation rate from the perched aquifer to the bedrock through the aquitard. Secondly, the sensitivity of the

* Corresponding author at: Department of Geography and Environmental Management, University of Waterloo, 200 University Ave. West, Waterloo, ON N2L 3G1, Canada. Tel.: +1 5198884567x32789.
E-mail address: mazdakompani@gmail.com (M. Kompanizare).

http://dx.doi.org/10.1016/j.advwatres.2014.08.006
0309-1708/

rate of bedrock recharge to the degree of bedrock depressurization, surface recharge rate and the surficial perched aquifer and aquitard hydraulic conductivities, were evaluated.

2. Study area

While the solutions presented are generally applicable to bedrock exposures or windows in confining layers, we present the results in the context of the peatlands surrounding the De Beers Victor mine in the James Bay Lowlands (JBL). In this area the peat layer thickness is 2–3 m, and is separated from the higher permeability fractured bedrock by an aquitard formed of fine-grained marine sediments (MS) [21–24]. The aquitard thickness is smaller or absent near bedrock exposures, locally present as bioherms (ancient coral reefs) [25], resulting in a zone of potentially high connectivity, if hydraulic gradients are present. Cropping and sub-cropping bioherms are present in 13% of the area, seated directly on the regional mid-Silurian limestone [26]. Exposed bioherms are circular domes [16] with elevations up to ~5 m above the surrounding peatland, typically about 100–150 m in diameter. In its undisturbed state this connection is unimportant, given the very low hydraulic gradients between the surface and deep aquifer. However, dewatering of an open-pit diamond mine (De Beers Victor mine) by pumping 80,000 to 120,000 m^3/day of groundwater from the bedrock aquifer [27], caused vertical gradients up to 0.45 in the vicinity of bioherms [28], resulting in local dewatering of the perched aquifer [29–32]. On and adjacent to exposed bioherms aquitard thickness is zero and gradually increases away from the exposure center. There exists a 10–80 m wide, "annular ring" of peat (perched aquifer) around bioherms laying directly over bedrock; beyond this the aquitard thickness increases from zero to more than 20 m at greater radial distances [25], although its thickness is highly variable because of the widespread presence of sub-cropping bioherm formations. Consequently, bioherms and adjacent areas with little or no aquitard can recharge up to several orders of magnitude more water than surrounding areas, especially in depressurization conditions [28]. The recharge rates around the bioherm mainly depend on the general form of exposure cross-section and consequently on the pattern of marine sediment thicknesses, which typically increase with radial distance from the bioherms. Given the depressurization of the regional aquifer, and the relatively high permeability of the bedrock exposure (0.01–3.7 m/day [27,33]) compared to the aquitard (2.5×10^{-5} to 0.5 m/day [33]), radial-symmetric flow occurs toward its exposure, similarly to flow toward a pumping well.

3. Theory and solutions

In this study the radially symmetric horizontal flow in a thin shallow perched aquifer (the peat layer around bioherms) and the vertical percolation rate through an aquitard layer (MS layer) toward the bedrock layer were solved for several sets of assumptions (Fig. 1). Solutions were sought for radial flow towards the bioherm with constant saturated thickness, and constant surface recharge and for different configurations of aquitard layer thickness (Fig. 2), including constant (MSn0, Fig. 2c) as well as linearly changing (MSn1, Fig. 2d) and quadratically changing (MSn2, Fig. 2e). In all solutions it is assumed that the perched aquifer has constant thickness and infinite extent and flow is radial and almost horizontal, whereas flow in the aquitard is vertical and downward (Figs. 1 and 2). In reality the flow in such a perched aquifer is not completely horizontal and is inclining downward, but because of its comparatively high hydraulic conductivity [25] its vertical component is assumed negligible compared with its horizontal component. The effect of vertical flow through the aquitard layer on the horizontal flow budget and its decreasing trend with radial distance in the perched aquifer was taken into account in this solution. The solutions were done for different cases of surface recharge, bedrock head and saturated thickness of flow in the perched aquifer and for different patterns of aquitard thickness. In these solutions the perched aquifer and aquitard layer are presumed to be saturated even when the water level in bedrock is below the bottom boundary of the aquitard layer. This type of perched saturated layer occurs where vertical downward flow in the fine-grained sediments overlaying a more permeable (e.g., fractured bedrock) layer is impeded by the capillary barrier effect [34].

The solutions presented in this paper predict the radial flow and vertical percolation around the bioherm exposure (Fig. 2a). They are applicable for the "main part" of the domain where the aquitard layer exists between the perched aquifer and bedrock (Fig. 2) and not applicable for the "central exposure" (see Fig. 2a) where neither perched aquifer nor the aquitard layer exist, nor the "annular ring" where the aquitard is absent. The vertical percolation rate from the perched aquifer to bedrock through the aquitard layer, and the horizontal flow passing through the perched aquifer from the "main part" (Fig. 2a) to the "annular ring" were determined with these solutions. Constant rate surface recharge was considered for all solutions. The first solution is analogous to that presented by Todd and Mays [35], who simulated the radial flow toward a pumping well (comparable with radial flow toward a bioherm), and is added here to compare its results, dimensionless curves and assumptions with our solutions. In the Todd and Mays solution (Fig. 2b) the percolation rate from the perched aquifer to bedrock is spatially constant. The second set of solutions is to test how variable thickness and configuration of the aquitard layer (Fig. 2c, d and e) affects the percolation losses away from the "central exposure". In these solutions the vertical percolation rate is controlled by the head difference between the perched aquifer and bedrock, aquitard thickness and aquitard hydraulic conductivity. The solutions were transformed to their dimensionless forms and their corresponding dimensionless curves were drawn. The variations in horizontal flow rate, vertical percolation rate through aquitard, ratio between horizontal and vertical velocities and gradients along the radial distance were also investigated.

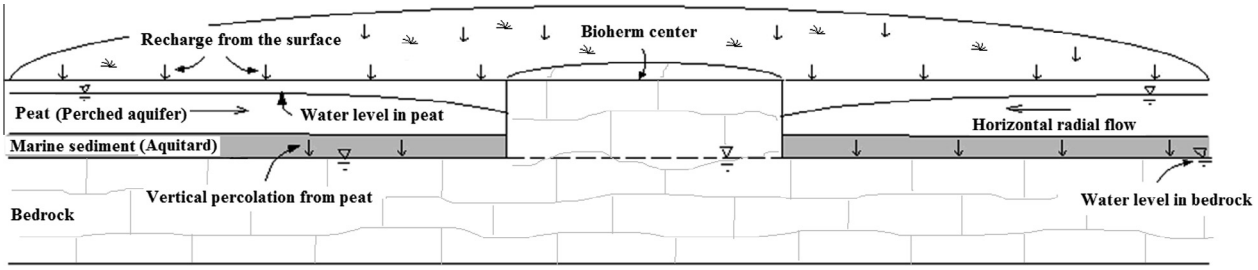

Fig. 1. The horizontal radial and vertical components of the flow in peat layer (perched aquifer) around a bioherm.

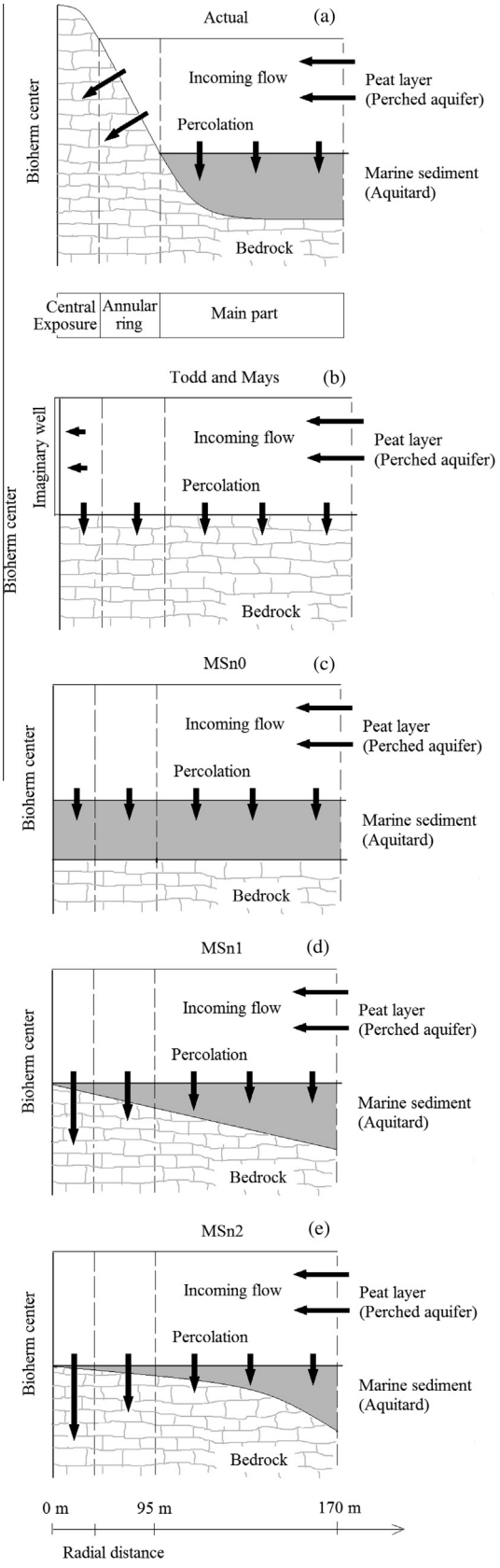

Fig. 2. Schematic section of peat, aquitard and bedrock layers for (a) the idealized geological profile; (b) the Todd and Mays solution and for various representations of marine sediment geometry (c) MSn0, (d) MSn1 and (e) MSn2 in them Eq. (8) was solved for $n = 0$, 1 and 2, respectively. Incoming flow and percolation rates and their relative values in different radial distances are illustrated schematically by arrows.

3.1. Todd and Mays [35] solution: constant vertical percolation rate

In this case the percolation rate from the perched aquifer to bedrock is assumed spatially constant. Also the surface recharge rates, in the form of rain, snowmelt or evapotranspiration can be assumed spatially constant regardless of the hydraulic characteristics of underlying layers. In the solution presented by Todd and Mays [35] a constant net surface recharge or discharge rate was added or subtracted from the radial flow toward the bioherm center along its path (Fig. 2b). The advantage of this solution is that the horizontal flow rate in the perched aquifer depends on both the net recharge rate as well as the exploitation rate from an imaginary vertical well at the center (Fig. 2b). For example if there is no net recharge to/from the perched aquifer, the horizontal flow rate would be spatially constant and equal to the flow rate toward the imaginary well. This case was solved assuming variably saturated thickness of horizontal-radial flow [35] in the perched aquifer.

The constant net recharge rate to the perched aquifer, $R(LT^{-1})$, can be determined by subtracting the vertical downward percolation rate through the aquitard layer, $w(LT^{-1})$ from the surface recharge rate, $W(LT^{-1})$ (Fig. 3). R is positive for inflow and negative for outflow from the perched aquifer. By considering the net recharge rate, R, the horizontal flow rate, Q, in a given section is

$$Q = Q_0 + (\pi r_0^2 - \pi r^2)R \tag{1}$$

where $Q(L^3T^{-1})$ is the horizontal flow rate, r (L) is radius from the bioherm center; K (LT^{-1}) is the perched aquifer horizontal hydraulic conductivity and Q_0 (L^3T^{-1}) is the horizontal flow rate entering the section at radial distance r_0(L). The calculated flow rate in Eq. (1) can be written as

$$Q_0 + (\pi r_0^2 - \pi r^2)R = 2\pi r K h \frac{dh}{dr} \tag{2}$$

in which h (L) is the saturated thickness of flow in the given section. Eq. (2) can be solved for the saturated thickness, h, which varies with radial distance, as

$$h = \left[\left(\frac{-[Q_0 \ln(\frac{r_0}{r})] - [R\pi r_0^2 \ln(\frac{r_0}{r})] + [R\pi(r_0^2 - r^2)/2]}{K\pi}\right) + h_0^2\right]^{0.5} \tag{3}$$

where h_0 (L) is the hydraulic head at radial distance r_0(L).

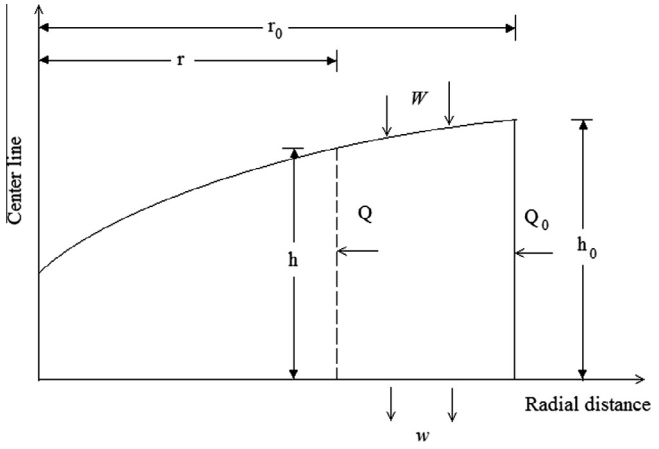

Fig. 3. The schematic flow domain in the peat layer for the Todd and Mays solution, in which the saturated thickness of flow in the perched aquifer (peat layer) is variable (h), but with constant vertical percolation (w).

3.2. Solutions for constant and variable aquitard layer thickness (MS solutions)

As discussed in the Todd and Mays solution, the MS solutions are for the "main part" of the perched aquifer in the flow domain (Fig. 2b, c, d and e). In this set of solutions the saturated thickness of flow in the perched aquifer, b, is constant (Fig. 4) and the percolation rate, w, through the aquitard is a function of the difference between heads in the perched aquifer and bedrock (h_1 and h_2, Fig. 4), the aquitard thickness, t, and aquitard vertical hydraulic conductivity. Here, the main controlling factor on vertical flow is the aquitard layer because of its low vertical hydraulic conductivity compared with the perched aquifer and bedrock. The head in the bedrock is presumed to be spatially constant as measured at the "central exposure". Also, it is assumed that there is a constant vertical recharge (W) from the surface to the perched aquifer that, along with the percolation loss (w), produces a net recharge, R (to or from the perched aquifer). In this solution flow in the "main part" of the perched aquifer is controlled either by the horizontal flows at 95 and 170 m radial distances and/or the net recharge, R, (Fig. 2c, d and e). In this solution the flow is radially symmetric, the only in- and out-flows are horizontal at the 95 and 170 m radial distances, as well as through the top and bottom boundaries (recharge from the top and percolation from the bottom). In this case, if R is equal to zero (no net flux across the top and bottom boundaries) then the horizontal incoming flow to the perched aquifer will be zero (i.e., it cannot accept any flow if it is not losing any). There is no imaginary well in the center to receive the excess flow as in the Todd and Mays solution. In this set of MS solutions, it is assumed that in a thin cylindrical control volume that represents flow between successive cylindrical rings in the perched aquifer (Fig. 4) (only two rings shown for illustrative purposes) the difference between the flow rates in two successive sections, $\Delta Q_1 = Q_1 - Q_2$, is equal to the vertical outflow percolating downward from that section, w_1 (Fig. 4). Then, the vertical flow rate in this section can be written based on the Darcy equation in the vertical direction as

$$2\pi r w_1 dr = 2\pi r K_v \frac{h_1 - H}{t} dr \tag{4}$$

in which $K_v(\mathrm{LT}^{-1})$ is the vertical hydraulic conductivity of aquitard, h_1 (L) is the average hydraulic head in the given control volume, t (L) is aquitard thickness, r(L) is the radial distance from middle of the given volume to the center, dr is the radial thickness of the control volume that is infinitely small and H (L) is the hydraulic head in bedrock which is assumed to be constant. To simplify the equations the water level in bedrock was assumed to be coincident with datum plain ($H = 0$). Based on the Darcy and continuity equations in the horizontal direction, ΔQ_1 can be written as

$$\Delta Q_1 = \frac{d}{dr}\left(2\pi r b K \frac{dh}{dr}\right) dr \tag{5}$$

By considering $H = 0$, Eqs. (4) and (5) can be merged to

$$2\pi r K_v \frac{h}{t} dr = \frac{d}{dr}\left(2\pi r K b \frac{dh}{dr}\right) dr. \tag{6}$$

For the condition where there is a constant vertical recharge from the surface, $W(\mathrm{LT}^{-1})$, the percolation rate in Eq. (6), $w = K_v \frac{h}{t}$, is replaced by the net vertical outflow rate which is the sum of the percolation rate and vertical recharge from the surface $\left(K_v \frac{h}{t} - W\right)$, and then Eq. (6) can be simplified to a form of a Modified Bessel function [36] as

$$r^2 h'' + r h' - r^2\left(\frac{h K_v}{K b t} - \frac{W}{K b}\right) = 0. \tag{7}$$

The minus sign before the W parameter in Eq. (7) is required because recharge from the surface flows into the perched aquifer and percolation flows out from it. The thickness of the aquitard, t, can increase radially and symmetrically with different orders (values of n) as presented in Appendix A, depending on the trend of changes in aquitard thickness outward from the bioherm. Therefore, t, in Eq. (7) can be replaced by Ar^n (Eq. A.1) so that

$$r^2 h'' + r h' - r^2\left(\frac{h K_v}{K b A r^n} - \frac{W}{K b}\right) = 0. \tag{8}$$

Eq. (8) can be solved for different n values. In solutions MSn0, MSn1 and MSn2, Eq. (8) was solved for $n = 0$, 1 and 2, respectively, as described below.

3.2.1. MSn0:n = 0, Constant thickness aquitard (see Fig. 2b)

Eq. (8) with $n = 0$ has a form of a Modified Bessel function. The solution for Eq. (8) with $n = 0$ is in the following form:

$$h = \left(\frac{h_1 - \frac{W A_{n0}}{K_v}}{\mathrm{I}_0\left(\sqrt{\frac{K_v}{K b A_{n0}}} r_1\right)}\right) \mathrm{I}_0\left(\sqrt{\frac{K_v}{K b A_{n0}}} r\right) + \frac{W A_{n0}}{K_v}, \tag{9}$$

in which h_1 is the head at a certain radius, r_1.

3.2.2. MSn1: n = 1, Linear increase of aquitard thickness (see Fig. 2c)

The solution for Eq. (8) with $n = 1$ is

$$h = \mathrm{I}_0\left(2\sqrt{\frac{K_v}{K b A_{n1}}}\sqrt{r}\right) \frac{\left(h_1 - \frac{W A_{n1}(K b A_{n1} + K_v r_1)}{K_v^2}\right)}{\mathrm{I}_0\left(2\sqrt{\frac{K_v}{K b A_{n1}}}\sqrt{r_1}\right)} + \frac{W A_{n1}(K b A_{n1} + K_v r)}{K_v^2}, \tag{10}$$

where A_{n1} corresponds to coefficient A in Eq. (A.1) for this Case, and h_1 is the head at a certain radius, r_1.

3.2.3. MSn2: n = 2, second order increase of aquitard thickness (see Fig. 2d)

The solution for Eq. (8) with $n = 2$ is

$$h = r^{\frac{\sqrt{K_v}}{\sqrt{K}\sqrt{b}\sqrt{A_{n2}}}} \left(\frac{-h_1 K_v + 4 h_1 K b A_{n2} + W A_{n2} r_1^2}{r_1^{\frac{\sqrt{K_v}}{\sqrt{K}\sqrt{b}\sqrt{A_{n2}}}} (-K_v + 4 K b A_{n2})}\right) - \frac{W A_{n2} r^2}{-K_v + 4 K b A_{n2}}, \tag{11}$$

where for this case A_{n2} is coefficient A in Eq. (A.1) and other variables are as previously defined.

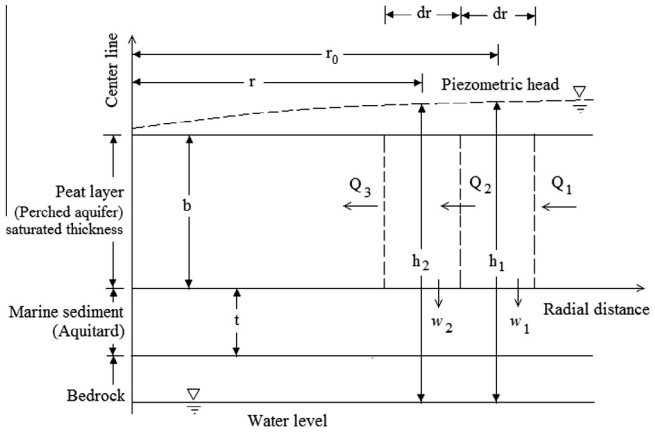

Fig. 4. The schematic flow domain in the peat layer (perched aquifer) for the MS solution, in which the saturated thickness of flow in the perched aquifer (b) is constant, and the vertical recharge or percolation rates (w) are variable. The vertical percolation rate is a function of the head difference between the peat and bedrock layers (h_1 or h_2), and MS (aquitard) thickness (t) and vertical hydraulic conductivity.

4. Results and discussions

4.1. Dimensionless solutions

As previously noted, to create more general solutions, and to be able to fit the curves to field data through optimization, dimensionless solutions (Table 1) and their corresponding curves were developed. By using these dimensionless variables, Eqs. (3), (9), (10) and (11) were transformed to their dimensionless forms (Table 2). For all such solutions, dimensionless head (h_D) versus dimensionless radius (r_D) cross each other at $h_D = 1$ and $r_D = 1$, which facilitates comparison of various values of R, W and dimensionless hydraulic conductivity ($KK_{n0}, KK_{n1}, KK_{n2}$).

4.1.1. Dimensionless curves

The dimensionless curves (Figs. 5 and 6) corresponding to the equations in Table 2, were drawn by using different dimensionless radii and dimensionless heads for the given parameter values. It should be noted that h_{rD} (Table 1) is the ratio between the average of heads and radii of all observation points. The constant saturated thickness of the perched aquifer here is assumed to be 2.41 m, which is equal to the average saturated thickness of perched aquifer in the 95–170 m interval, based on the field values.

It was found that some of the dimensionless variables consistently used in the form of a ratio could be replaced by a single variable to facilitate parameter optimization and fitting of the dimensionless curves to field data. For MSn0, MSn1 and MSn2 the combined variables are $KK_{n0} = \frac{K_{vD}}{A_{n0D}}$, $KK_{n1} = \frac{K_{vD}}{A_{n1D}}$ and $KK_{n2} = \frac{K_{vD}}{A_{n2D}}$, which are a combination of dimensionless hydraulic conductivity and the thickness coefficient for aquitard. The dimensionless curves can also be plotted according to their combined dimensionless variables rather than their individual dimensionless variables.

To plot the field data on dimensionless curves the data points were transformed to their dimensionless values using the equations in Table 1. Similarly, the heads and radii of observation wells were normalized by the selected radius and head. Here the selected radius and head were the average values of the heads and radii of the observation boreholes. The head values for the Todd and Mays solution were the difference between the head in observation wells and the bottom of the perched aquifer, and for the MS solutions was the difference between the heads in perched aquifer and the bedrock. For the solutions of MSn0, MSn1 and MSn2 the constant perched aquifer saturated thickness is 2.41 m, as noted above. For all cases the average hydraulic conductivity of the perched aquifer, K, is assumed to be 0.27 m/day [25,28].

To illustrate the fitting of the dimensionless curves and field data the dimensionless curves were plotted (Figs. 5 and 6) beside the field data (in dimensionless form) for June 27, 2012 (P. Whittington, unpublished data), for the "North Bioherm" (see [25,28]). On this date the water level in all mine-impacted peatland boreholes (M. Leclair, pers. comm.) were relatively steady, and representative of the 2012 summer period; during this period the average monthly surface recharge was 1.2×10^{-3} m/day. It should be noted that based on the previous work on the North Bioherm [25], at some observation points closer than about 90 m to the bioherm, the perched aquifer directly overlays the bedrock, where the MS solutions assumptions are not applicable. Therefore, the observation points further than 90 m from the bioherm center (bore holes along transect 8 presented by Whittington and Price [25]), were used in our calculations. In this transect r_1 (Table 1) is 132.57 m and h_1 (the average head) for the Todd and Mays as well as MS solutions was 2.41 m and 8.97 m, respectively.

4.1.1.1. Dimensionless curves for the Todd and Mays solution. For the Todd and Mays solution, dimensionless curves of heads versus radial distance were drawn for different values of dimensionless net recharge rate, R_D (Fig. 5). Curves with negative R_D values (net discharge) are concave upward, while the curves with positive R_D values (net recharge) are convex upward. Also, for the curve with $R_D = 0$, a small upward convexity occurs, due to radial flow in which there is a decrease in flow cross-section and thus increase in hydraulic gradients toward the bioherm center. For conditions with negative R_D values, the horizontal flow rate and horizontal hydraulic gradient at relatively large dimensionless radial distances are decreasing toward the bioherm center and approaching the point with zero gradient and zero horizontal flow rate. At smaller radial distances, the horizontal flow is outward from the bioherm. In contrast, for cases with positive R_D the heads in the perched aquifer peak at dimensionless radial distance >1, representing a water divide; peak values are closer to the bioherm with successively higher R_D. The field data for 27 June, 2012 are plotted in Fig. 5. This illustrates flow toward the bioherm, with water divide at r_D = 5.17 (r = 686 m). The points were fitted using the optimization routine in Maple®; the best fit was at $R_D = 3.34 \times 10^{-6}$. The root mean squared (RMS) value, in the range of 7.18×10^{-5} to 1.27×10^{-2}, for the fitted curve is presented in Table B.1.

4.1.1.2. Dimensionless curves for the MS solutions. Fig. 6a–f shows the dimensionless curves of head versus radial distance for MSn0, MSn1 and MSn2 solutions and June 27, 2012 field data. The curves are drawn for a range of dimensionless aquitard hydraulic conductivity ($KK_{n\#}$) and surface recharge (W_D) as they vary over a range of aquitard thicknesses (i.e., associated with their respective n parameter). The curves in Fig. 6a, c and e are drawn for $W_D = 4.45 \times 10^{-3}$ (corresponding to dimensional surface recharge of 1.2×10^{-3} m/day) and for different values of KK_{n0}, KK_{n1} and KK_{n2} (dimensionless vertical hydraulic conductivity for unit

Table 1
Dimensionless variables and their equations showing their relations to their corresponding dimensional variables. Subscript D refers to the dimensionless form. Subscripts $n0, n1$ and $n2$ are for solutions with orders zero, one and two, respectively. For example A_{n1} is the thickness coefficient for $n1$.

Dimensionless variable	Equation	Dimensionless variable	Equation
Thickness coefficient for zero order	$A_{n0D} = A_{n0}/h_1$ (MSn0)	Aquitard conductance coefficient for first order	$KK_{n1} = \frac{K_{vD}}{A_{n1D}}$
Thickness coefficient for first order	$A_{n1D} = A_{n1}$ (MSn1)	Aquitard conductance coefficient for second order	$KK_{n2} = \frac{K_{vD}}{A_{n2D}}$
Thickness coefficient for second order	$A_{n2D} = A_{n2}h_1$ (MSn2)	Horizontal flow rate in Todd and Mays solution	$Q_D = Q/2\pi h_1 K r_1$ (Todd and Mays solution)
Perched layer saturated thickness	$b_D = b/r_1$	Horizontal flow rate in certain radius in Todd and Mays solution	$Q_{1D} = Q_1/2\pi h_1 K r_1$ (Todd and Mays solution)
Head difference between perched layer and bedrock	$h_D = h/h_1$ (MS solution)	Radial distance	$r_D = r/r_1$
Selected head and selected radius ratio	$h_{rD} = h_1/r_1$	Surface recharge rate	$W_D = W/K$
Vertical hydraulic conductivity in aquitard	$K_{vD} = K_v/K$	Net recharge rate	$R_D = R/K$
Aquitard conductance coefficient for zero order	$KK_{n0} = \frac{K_{vD}}{A_{n0D}}$		

Table 2
Dimensionless equations for Todd and Mays solution, MSn0, MSn1 and MSn2 (Eqs. 3, 9, 10 and 11, respectively) based on the dimensionless variables presented in Table 1.

Case	Descriptions	Dimensionless equation
Todd and Mays	Constant percolation rate Variable saturate thickness flow	$h_D = \left[1 - \left(\left[\frac{2Q_{1D}}{h_{rD}}\ln\left(\frac{1}{r_D}\right)\right] - \left[R_D\frac{1}{h_{rD}^2}\ln\left(\frac{1}{r_D}\right)\right] + \frac{1}{h_{rD}^2}\left[R_D(1-r_D^2)/2\right]\right)\right]^{1/2}$
MSn0	Constant thickness of aquitard ($n = 0$) Percolation rate depends on head difference between perched aquifer and bedrock, aquitard hydraulic conductivity and thickness	$h_D = \left(\frac{1-\frac{W_D}{KK_{n0}}}{I_0\left(\sqrt{\frac{KK_{n0}}{b_D h_{rD}}}\right)}\right) I_0\left(\sqrt{\frac{KK_{n0}}{b_D h_{rD}}}r_D\right) + \frac{W_D}{KK_{n0}}$
MSn1	Linearly increasing aquitard thickness ($n = 1$) Percolation rate depends on head difference between perched aquifer and bedrock, aquitard hydraulic conductivity and thickness	$h_D = I_0\left(2\sqrt{\frac{KK_{n1}}{b_D}}\sqrt{r_D}\right)\frac{\left(1-\frac{W_D}{KK_{n1}}\left(\frac{b_D}{h_{rD}}+1\right)\right)}{I_0\left(2\sqrt{\frac{KK_{n1}}{b_D}}\right)} + \frac{\frac{W_D}{KK_{n1}}\left(\frac{b_D}{h_{rD}}+r_D\right)}{h_{rD}}$
MSn2	Second order increase in aquitard thickness ($n = 2$) Percolation rate depends on head difference between perched aquifer and bedrock, aquitard hydraulic conductivity and thickness	$h_D = r_D^{\frac{\sqrt{KK_{n2}}\sqrt{h_{rD}}}{\sqrt{b_D}}}\left(\frac{-KK_{n2}+\frac{4b_D}{h_{rD}}+\frac{W_D}{h_{rD}^2}}{\left(-KK_{n2}+\frac{4b_D}{h_{rD}}\right)}\right) - \frac{W_D r_D^2}{h_{rD}^2\left(-KK_{n2}+\frac{4b_D}{h_{rD}}\right)}$

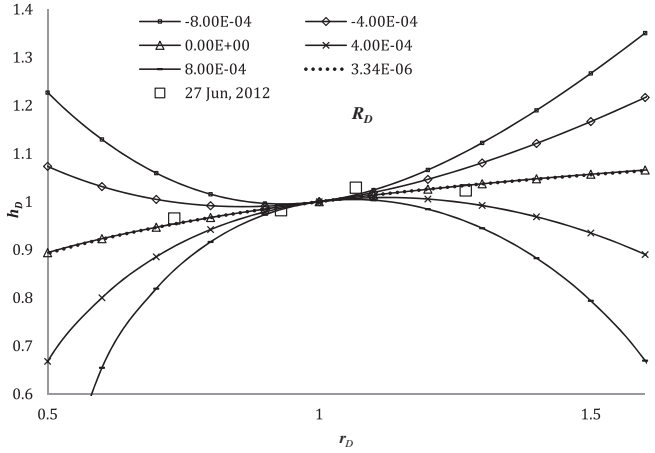

Fig. 5. Dimensionless curves for the Todd and Mays solution and for different R_D values beside the field data for June 27, 2012. Variable are h_D (dimensionless head), r_D (dimensionless radius) and R_D (dimensionless recharge rate). The best fit value is $R_D = 3.34e{-}6$.

dimensionless thickness coefficient, or transmission rate ratio), respectively. Fig. 6b, d and f are drawn for the optimum values of $KK_{n0} = 4.55 \times 10^{-3}, KK_{n1} = 4.37 \times 10^{-2}$ and $KK_{n2} = 3.89 \times 10^{-1}$, respectively, and different values of W_D.

Fig. 6a, c and e are drawn for the aquitard thickness functions of zero, first and second orders, or $n = 0$, 1 and 2, respectively that are illustrated in Fig. 2. In MSn0 (Fig. 6a) the aquitard layer thickness is constant and by increasing KK_{n0} the slope of the curves change from decreasing with radial distance from the bioherm, to sloping toward it. This is because increases in the transmission ratio, KK_{n0}, either due to higher aquitard hydraulic conductivity or smaller aquitard thickness, cause an increase in percolation rate to the bedrock hence greater horizontal flow toward the bioherm. For smaller KK_{n0} values the percolation rate is lower so higher head is maintained and thus the capacity of the bioherm to receive horizontal flow is small and the surface recharge flows outward. In Fig. 6a the curves with outward slopes are convex upward and the curves with slopes toward the bioherm are concave upward. The smaller absolute slope of the curves in the smaller radial distances is because in both inward and outward horizontal flow scenarios the flow rate in the bioherm center is zero. In the outward flow solution the surface recharge rate is greater than the percolation rate so horizontal flow increases outward. In contrast, with inward horizontal flow the surface recharge rate is less than the percolation rate so the flow decreases toward the bioherm.

In Fig. 6c and e, the curves are convex upward and those with higher transmission ratios (KK_{n1} and KK_{n2}) have an obvious peak or water divide. The slope of the curves (thus flow rate) increases with distance from the water divide. If visualized in three dimensions the water divide points would form a circle around the bioherm representing a water capture zone, within which the recharging water flows toward the bioherm, and beyond which flows outward. In Fig. 6c and e, with increasing KK_{n1} and KK_{n2} the water divides shifts toward larger radii, r_D, from 0 to about 1.5 (i.e., the capture radius of the bioherm increases).

Fig. 6b, d and f are drawn for constant and optimum values of KK_{n0}, KK_{n1} and KK_{n2} and different values of W_D that range from negative (discharge) to positive (recharge). The shapes of the curves in Fig. 6b are distinctly different from those in 6d and f. In Fig. 6b (solution for MSn0; constant aquitard thickness) the curves change with increasing recharge rates, W_D, from sloping toward the bioherm center to outward from it, and with upward concave curvature to convex upward curvature. In the case of negative surface recharge (discharge) the flow has a decreasing trend and is toward the bioherm center (i.e., less flow passes horizontally through the perched aquifer). For dimensionless surface recharge higher than 4.45×10^{-3} (i.e. equivalent to actual recharge of 1.2×10^{-3} m/day), the excess water flows outward, away from the bioherm. In Fig. 6d and f the curves with W_D less than 4.45×10^{-3}, or negative net recharge, are sloping toward the bioherm and in curves with positive net recharge there is a peak or water divide.

The curves fitted to the dimensionless observed heads versus radial distances for four boreholes along transect 8 (Appendix B) are illustrated in Fig. 6. The root mean square (RMS) values of the fits are shown in Table B.1. The RMS and plots illustrate that the only acceptable fit is for the case MSn0 (RMS of 7.18×10^{-5}). For the MSn1 and MSn2 the fitted curves do not match the observed points. A plausible interpretation of the better fit of the observation points to the MSn0 curves, is that there is actually a more uniform distribution of aquitard thickness, and consequently percolation rates, along the radial distance. Alternatively, in spite of subtle fluctuations in aquitard thickness that almost certainly occur in the field, the transmissivity of the aquitard, for a given head gradient, is controlled by the ratio K_v/t (vertical hydraulic conductivity to thickness of the aquitard) [28], which may be more homogenous than t, alone.

4.2. Dimensional variables

The dimensionless and dimensional variables for the Todd and Mays as well as MSn0 solutions that produced the best fit with field data (Figs. 5, 6a and b), are discussed further. The horizontal flow rate, Q, in each radius was determined based on the derivative of head on the given radius (Eqs. 1, 3, 9, 10 and 11), and vertical gradients and velocities in each radius were calculated based on the difference between heads in the perched aquifer and bedrock

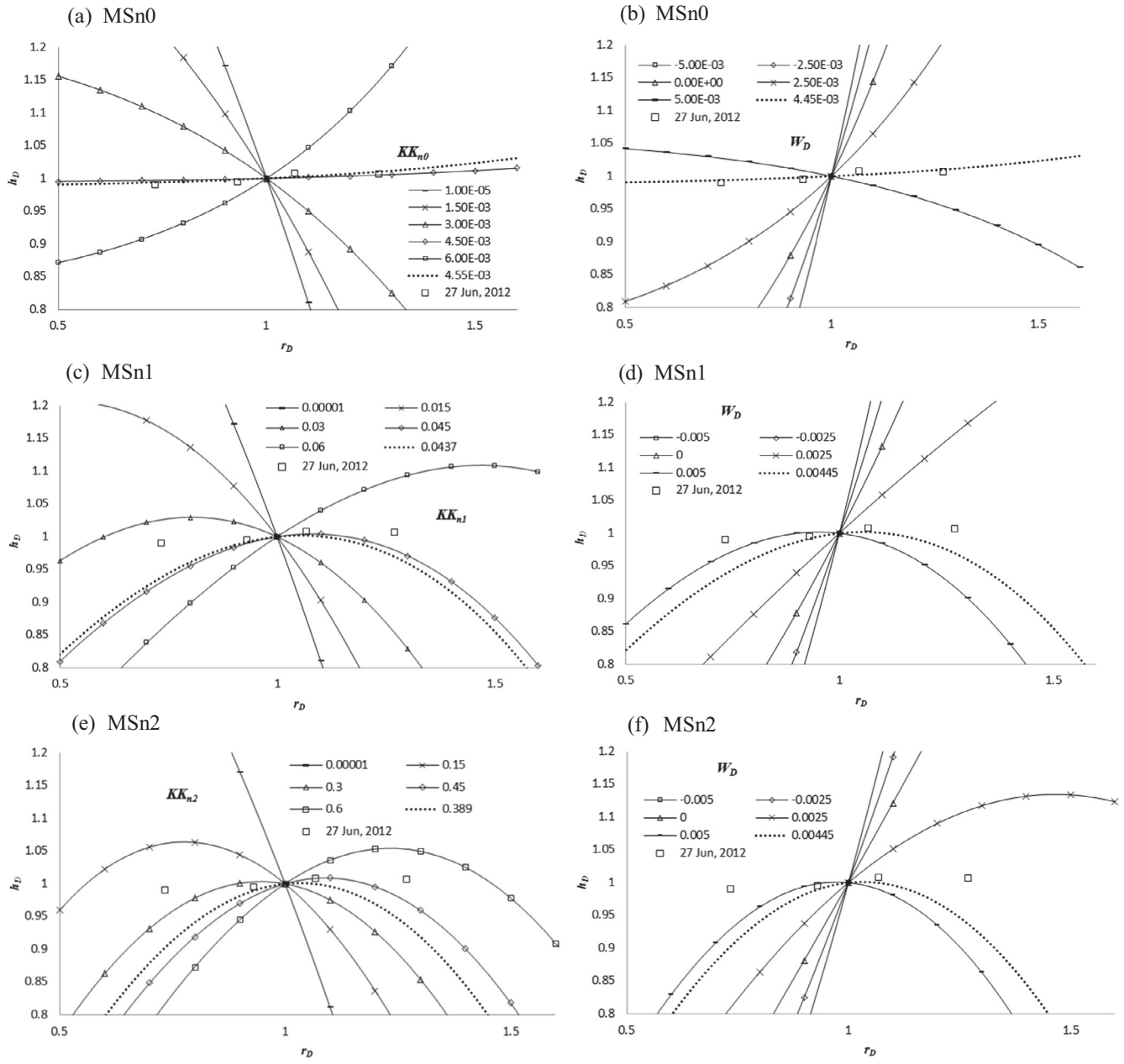

Fig. 6. Dimensionless curves for MSn0 (a and b), MSn1 (c and d), and MSn2 (e and f) for a constant value of dimensionless surface recharge, W_D= 4.45e−3 and different values of relative hydraulic conductivity, KK_{n0}, KK_{n1}, KK_{n2} (a,c,e); and for the cases of constant and optimum values of KK_{n0} = 4.55e−3, KK_{n1} = 4.37e−2, KK_{n2} = 3.89e−1 and various values for W_D (b,d,f). The curves were fitted to the observation points of transect 8 for June 27.

and the aquitard thickness, as discussed for Eq. (4). The surface recharge was determined based on the monthly average of precipitation minus evapotranspiration, P−E of 1.2×10^{-3} m/day (Leclair, M., and Price, J., unpublished data), for June 27, 2012.

In the third and fourth columns of Table 3, ΔQ is the difference between the horizontal flow rates at radius 170 and 95 m and Q_f is the horizontal flow rate at radius 95 m, toward the bioherm center from the "main part" to the "annular ring" (Fig. 2). Therefore, the total horizontal flow rate in the perched aquifer toward the bioherm at radius 170 m is equal to $Q_f - \Delta Q$. As can be seen in Table 3 for the Todd and Mays as well as MS solutions, respectively, Q_f values are 1.31 and 0.49 m^3/day and ΔQ values are 0.05 and −1.79 m^3/day. Thus in the Todd and Mays solution the horizontal flow in the radial interval between 95 and 170 m increases toward the bioherm center, while for the MS solution it decreases. The results of the two methods (Table 3) show that almost all of the surface recharge (Col. 12) percolated down through the aquitard layer, at a negligibly different rate ($\bar{w} = 1.19 \times 10^{-3}$ and 1.23×10^{-3} m/day). Additionally, both methods reveal that the horizontal flow rate through the perched aquifer at radial distance of 95 m (Q_f) is remarkably small and toward the bioherm (Col. 4). However, in the MS solution the negative net recharge, R, (shown by ΔQ = −1.79 m3/day, Col. 3, Table 3) points to a gradual decrease in the horizontal flow rate toward the bioherm, whereas the positive R value in the Todd and Mays solution (shown by ΔQ = 0.05 m3/day, Col. 3, Table 3) indicates a small increase.

K_v (vertical hydraulic conductivity in aquitard layer) and A_{n0} (aquitard thickness coefficients) were calculated, alternatively, based on the known value of each other (see Appendix C). The results of the two approaches where either K_v was the known variable ("Known K_v") or where A_{n0} was the known variable ("Known A_{n0}"), the resultant A_{n0}, K_v and R_G (horizontal to vertical gradient

Table B.1
The optimum dimensionless variables and combined variables beside their corresponding optimum values for the dimensional variables by considering $K = 0.27$ m/day.

Cases	Optimum dimensionless variables		RMS	Optimum dimensional variables based on $K = 0.27$ m/day	
	Q_{1D}	R_D		Q_1	R
Todd and Mays	2.27×10^{-3}	3.34×10^{-6}	2.32×10^{-3}	1.28	9.02×10^{-7}
	KK	W_D		K_v/A[a]	W
MSn0	4.55×10^{-3}	4.45×10^{-3}	7.18×10^{-5}	1.37×10^{-4}	1.2×10^{-3}
MSn1	4.37×10^{-2}	4.45×10^{-3}	4.17×10^{-3}	1.18×10^{-2}	1.2×10^{-3}
MSn2	3.89×10^{-1}	4.45×10^{-3}	1.27×10^{-2}	9.42×10^{-1}	1.2×10^{-3}

[a] K_v/A are $K_v/A_{n0}, K_v/A_{n0}$ and K_v/A_{n0} corresponding to their cases including MSn0, MSn1 and MSn2, respectively.

ratio) values are presented in Table 3 (columns 5 to 10). By using the measured value for K_v of 1.0×10^{-4} m/day, in the "Known K_v" approach (columns 5 and 6 in Table 3), A_{n0} was determined as 0.73 m. Similarly, by using the fitted value of A_{n0} (aquitard thickness) equal to 1.2 m in the "Known A_{n0}", K_v was calculated as 1.6×10^{-4} m/day (columns 8 and 9 in Table 3). It was found that A_{n0}, K_v and R_G values in the two approaches (Known K_v and Known A_{n0}) were almost the same.

The smaller value of 1.77×10^{-4} for R_G (ratio between horizontal and vertical gradients) in the first approach (Col. 7, Table 3) compared to 2.7×10^{-4}, in the second approach (Col. 10, Table 3), is due to the comparatively smaller values for K_v and A_{n0} in the first approach. The value (horizontal to vertical velocity ratio) of 0.47, reflects the smaller horizontal velocity in comparison with vertical velocity in the MSn0 case. This occurs because of the comparatively large hydraulic conductivity and very small gradient in the horizontal direction, compared to the relatively small hydraulic conductivity and huge gradient in the vertical direction. The value of R_V is independent of the approach used to determine K_v and A_{n0}.

The average percolation rate through the aquitard layer in the interval between 95 and 170 m, $\bar{w}$, (column 12, Table 3) is the average of the vertical percolation rates, w, in this interval. The vertical percolation rate at each radial distance in the Todd and Mays solution was determined by subtracting the constant surface recharge, W (based on P−E), from the calculated net recharge, R (Eq. 3); for the MSn0 solution$w$ was determined by Eq. 4. The average percolation rates determined from the Todd and Mays as well as MSn0 solutions are very similar (Table 3) at $\sim 1.2 \times 10^{-3}$ m/day, which is approximately 440 mm/y (if it is assumed recharge is negligible during the ~6 months frozen season, this would be ~220 mm/y); either value is higher than the range of 2.6 to 26 mm/y reported for pre-mining conditions (HCI [33]; Table B-8).

The similarity in the estimated percolation rates for the Todd and Mays as well as MSn0 solutions, which are independent and dependent, respectively, on the hydraulic characteristics of the underlying layer, lends support to the validity of the estimate. In following sections the variations of hydraulic head, h; percolation rate through aquitard, w; and horizontal discharge rate in the perched aquifer, Q, versus radial distance, for the MSn0 and Todd and Mays cases are discussed.

4.2.1. Hydraulic head

The MSn0 as well as Todd and Mays solutions are fitted to head data for June 27, 2012 in Transect 8 [25] next to the Northern bioherm (Fig. 7). There is a good match between the plotted points and the curves for both methods, in the 95–170 m interval. The difference between the curves in 0 to 90 m interval reflects the different assumptions associated with the respective methods. In the MSn0 solution the horizontal flow approaches zero toward the center (curve almost flat), whereas in the Todd and Mays solution the flow rate and its relevant drawdown remains above zero (curve relatively steep) close to the center, due to the assumption of an imaginary well (Fig. 2b). Hence, in the Todd and Mays solution an excess amount of flow reaches the center ($r = 0$) and the water was not completely gained by percolation through the bottom en route to the center. The water divide, or where the slope of the water level in the Todd and Mays solution is zero, is located at radius of 686 m. This radial distance is the capture zone of the northern bioherm when there is a recharge rate of 1.2×10^{-3} m/day. The head data in radial distance of 95 to 170 m were compared with numerical simulation results (Fig. 7). There is a good match between the numerical results determined with Hydrus 3D (Appendix D). The negligible difference between the MSn0 and numerical results is mainly due to the assumption of constant saturated thickness for the perched aquifer.

4.2.2. Horizontal discharge rate

Fig. 8 shows the horizontal discharge towards the bioherm (calculated according to saturated thickness and hydraulic gradient in each section) in the perched aquifer in the radial interval of 0–170 m for the MSn0 and Todd and Mays solutions (whose head values fit strongly – see Figs. 5 and 6). In the MSn0 solution the horizontal flow rate decreases toward the bioherm center, from 2.5 to 0 m^3/day, and in Todd and Mays solution is almost constant at 1.35 m^3/day. These patterns occur because the net recharge rate, R (Eq. (1)), in the MSn0 solution is -3.0×10^{-5} m/day (water loss) and in the Todd and Mays solution is 9.02×10^{-7} m/day (water gain) ($\bar{w} - W$, Table 3). Thus, the horizontal flow rate in the Todd and Mays solution is increasing toward the bioherm at a very small rate, and the total remaining flow rate is gained in the center by the imaginary well. Another point is that the average horizontal flow rates in the interval 95–170 m for both MSn0 and Todd and Mays

Table 3
The result of fitting curves for Todd and Mays as well as MSn0 Cases and their related parameters ($K = 0.27$ m/day). The variable are surface recharge, W; total resultant out-flow, ΔQ; horizontal flow rate to the bioherm passing through the radial distance of 95 m, Q_f; vertical hydraulic conductivity in aquitard, K_v; horizontal to vertical gradient ratio, for two approaches of known and values; horizontal to vertical velocity ratio, R_V; and the average vertical percolation rate, $\bar{w}$ in the radial interval of 95 to 170 m.

Case	$W_{(\frac{m}{day})}$	$\Delta Q_{(\frac{m^3}{day})}$	$Q_{f(\frac{m^3}{day})}$	Known K_v (Appendix C)			Known A_{n0} (Appendix C)			R_V	$\bar{w}_{(\frac{m}{day})}$
				$K_{v(\frac{m}{day})}$	A_{n0}	R_G	$K_{v(\frac{m}{day})}$	A_{n0}	R_G		
Col. 1	Col. 2	Col. 3	Col. 4	Col. 5	Col. 6	Col. 7	Col. 8	Col. 9	Col. 10	Col. 11	Col. 12
Todd and Mays	1.20×10^{-3}	0.05	1.31	–	–	–	–	–	–	–	1.19×10^{-3}
MSn0	1.20×10^{-3}	−1.79	0.49	1×10^{-4}	0.73	1.77×10^{-4}	1.6×10^{-4}	1.2	2.7×10^{-4}	0.48	1.23×10^{-3}

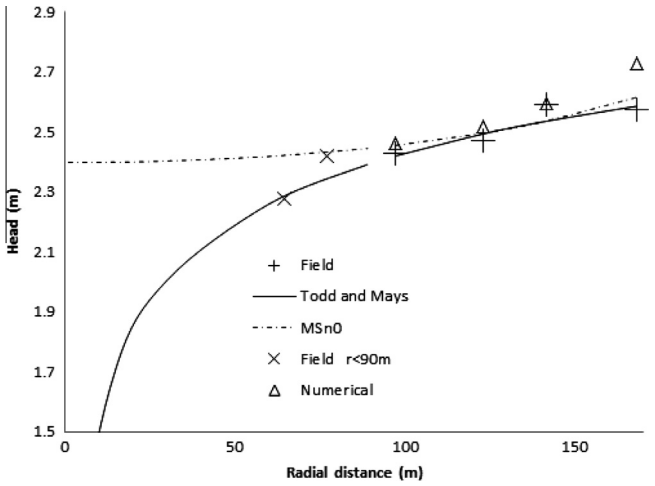

Fig. 7. Variation of hydraulic head h along radial distance, r, for the field data of June 27, 2012, with the curves for the Todd and Mays as well as MSn0 solutions.

methods are similar (the curves intersect at ~140 m), consequently, the fitted and observed head values (Fig. 7) are almost the same.

4.3. Effect of different parameters on percolation and horizontal flow rates

The MSn0 solution was used to determine the variation of the percolation (Fig. 9) and horizontal flow rates (Fig. 10) in the perched aquifer for aquitard layer thicknesses up to ~5 m. The curves were drawn for various head differences between the perched aquifer and bedrock, h (Eq. 6) (Figs. 9a and 10a); vertical hydraulic conductivity in the aquitard layer, K_v (Figs. 9b and 10b); horizontal hydraulic conductivity in the perched aquifer, K (Figs. 9c and 10c); and recharge rate from the surface, W (Figs. 9d and 10d). In these figures the percolation rate and the horizontal flow rates are calculated for the radial distances of 97 and 170 m, respectively. The common pattern evident in all cases is that there is a decrease in percolation rates and horizontal flow rates as the aquitard layer thickness increases. Furthermore, in most cases the slopes of change in flow rates with aquitard thickness are higher where the aquitard layer is thin and gradually decrease as the aquitard layer thickens. Another common point is that there is an aquitard layer thickness at which the percolation rate is equal to surface recharge, 1.2×10^{-3} m/day (Fig. 9a, b, and c), which corresponds to zero horizontal flow rate in the perched aquifer (see corresponding curves in Fig. 10a, b and c). This aquitard layer thickness is the critical thickness on which the net recharge rate, R (Eq. 1), to the perched aquifer is zero (Fig. 10a, b and c). In aquitard layer thicknesses less than this critical value the horizontal flow in perched aquifer is toward the bioherm and the bioherm is active in gaining water from the surrounding parts (Fig. 6a, $KK_{n0} = 6.0 \times 10^{-3}$) and for the thicknesses higher than that the horizontal flow is outward from the bioherm, and the bioherm is inactive (Fig. 6a, $KK_{n0} = 3.0 \times 10^{-3}$). In Figs. 9 and 10, it can be seen that for aquitard thicknesses smaller than the critical value, the percolation rate and horizontal flow rate toward the bioherm are remarkably more sensitive to aquitard thickness.

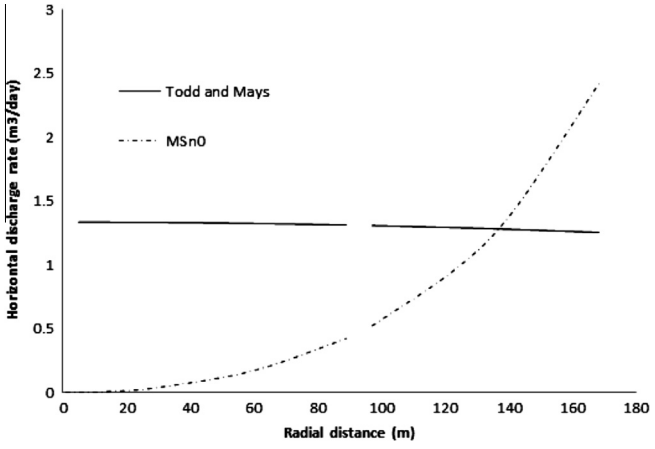

Fig. 8. Variation of horizontal discharge rate, Q, versus radial distance, r, for the Todd and Mays as well as MSn0 solutions fitted to heads on June 27, 2012 (Figs. 5 and 6).

4.3.1. The effect of head difference between the perched aquifer and bedrock

Fig. 9a shows that by doubling the head difference between the perched aquifer and bedrock, h_1, from 8 to 16 m, the percolation rates increases by an average of 1.7 times. Reducing the head difference to the situation that was presented before mine dewatering, from 8 to 2 m, the percolation rate reduces to about 0.45 times. The non-proportional change is a result of the changes in heads in the perched aquifer along the radial distance toward the bioherm caused by the percolation losses as well as the radial flow. The progressively different hydraulic gradients in the perched aquifer that occur along the radial distance towards the bioherm creates a non-linear change in the percolation rate.

The effect of head differences on horizontal flow rates in the perched aquifer is illustrated in Fig. 10a. By increasing head differences, the critical aquitard thicknesses (where horizontal flow goes to zero) shift to larger values. For example, for head difference of 2 m the bioherm is inactive for almost all aquitard layer thicknesses. This means that in pre-mining conditions, the head difference of 2 m, and with surface recharge, P–E, of 1.2×10^{-3} m/day, the northern bioherm had no contribution on collection of water from surrounding parts. However, for a head difference of 16 m the bioherm is active (gaining water) where aquitard thickness is less than about 1.4 m.

4.3.2. The effect of vertical hydraulic conductivity of the aquitard layer

Fig. 9b shows that by increasing K_v 10-fold, from 1.0×10^{-4} to 1.0×10^{-3} m/day, the percolation rates increase 1.3 and 6.7 times for aquitard thicknesses of 0.2 and 5.2 m, respectively. The corresponding values when K_v is increased from 1.0×10^{-5} to 1.0×10^{-4} are 4.9 and 9.4 times, respectively. This means that where the aquitard layer is thicker and K_v values are smaller, the percolation rates are more sensitive to K_v.

Fig. 10b shows that by increasing K_v from 1.0×10^{-4} to 1.0×10^{-3} m/day the critical aquitard layer thickness grows to more than 7 m. In this case a large area around the bioherm with aquitard thickness less than 7 m would be permeable similarly to the bioherm. However, for K_v of 1.0×10^{-5} m/day the critical aquitard layer approaches zero and the bioherm is not active even for MS thickness approaching zero.

4.3.3. The effect of horizontal hydraulic conductivity in the perched aquifer

In Fig. 9c the curves are drawn for different values of horizontal hydraulic conductivities in the perched aquifer. The curves here intersect at aquitard thickness of about 0.7. This occurs because in each case K_v and h_1 and W are the same and consequently the critical percolation rate would occur with the same aquitard layer thickness (Fig. 10c). For higher K values and consequently smaller horizontal gradients, the heads in the perched aquifer at different radial distances are more uniform, and adequately available to supply percolation. With higher K values, both the controlling effect of

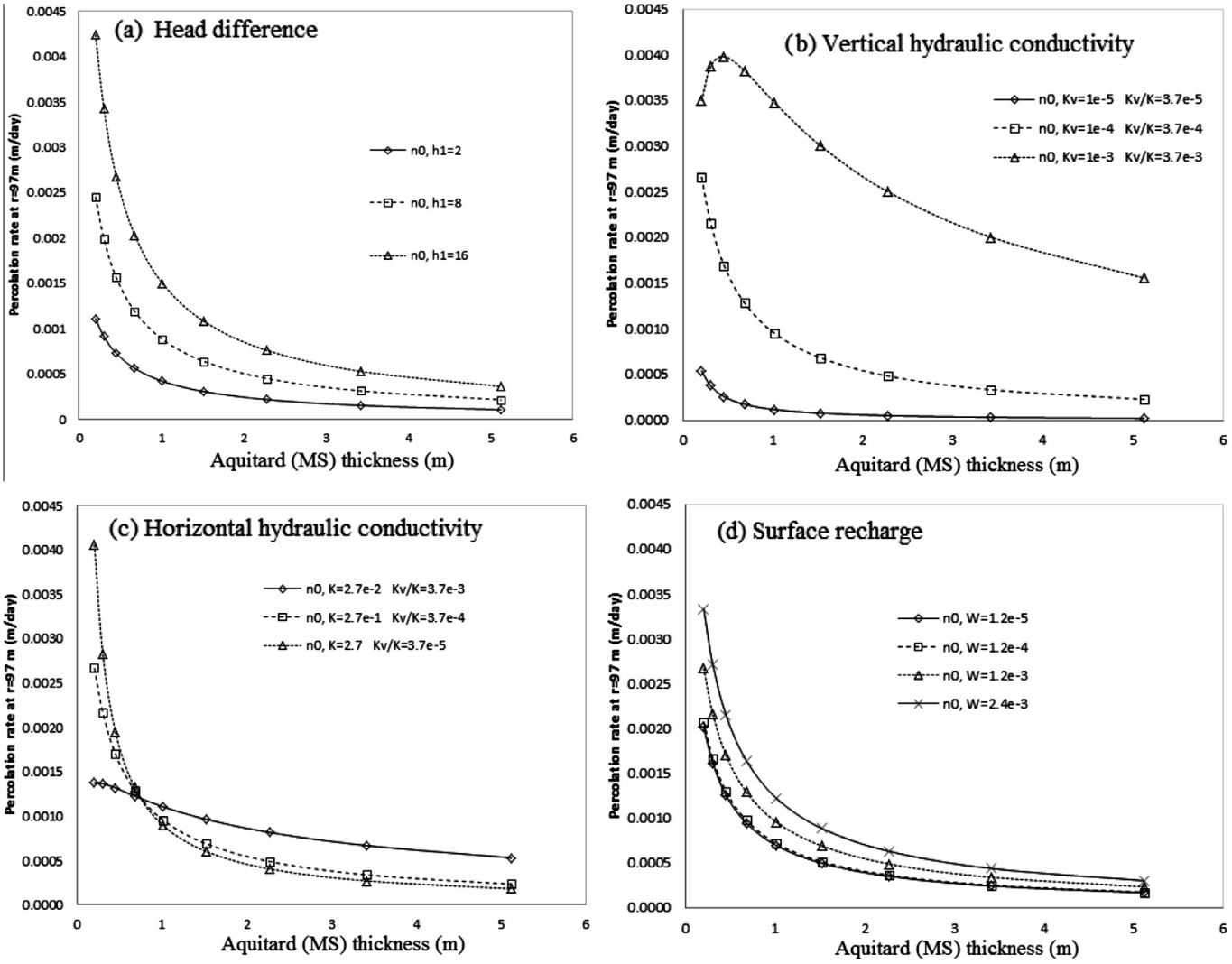

Fig. 9. Variations of percolation rate (m/day) versus aquitard layer thickness at $r = 97$ m, for various (a) head difference (h1) values between the perched aquifer and bedrock in m, (b) vertical hydraulic conductivity in aquitard layer (K_v), in m/day, (c) horizontal hydraulic conductivity in perched aquifer (K), in m/day and (d) recharge rate from surface, W, in m/day, by the MSn0 solution.

aquitard thickness on the percolation rate and the role of a bioherm with thinner aquitard in the collection of water would be magnified (Fig. 9c). Insensitivity of the horizontal flow rates to the K value in the perched aquifer and overlaying of curves with different K value in Fig. 10c is due to the similarity of the average head difference between the perched aquifer and bedrock in different cases.

4.3.4. The effect of surface recharge rates

The curves depicting the effect of surface recharge rates on percolation through the aquitard layer of differing thicknesses (Fig. 9d) are parallel and illustrate higher percolation rates correspond to higher surface recharge rates. Doubling the surface recharge rates from 1.2×10^{-3} to 2.4×10^{-3} m/day increases the percolation rates by a factor of 1.27; increasing the surface recharge 10-fold from 1.2×10^{-5} to 1.2×10^{-4} and from 1.2×10^{-4} to 1.2×10^{-3} m/day increases the percolation rates by 1.03 and 1.33 times, respectively. The percolation rates are more sensitive to surface recharge rates larger than 1.2×10^{-4} m/day. For this rate the percolation rates approach a minimum of about 9.7×10^{-4} m/day (for critical aquitard thickness of 0.7 m), which is independent of the surface recharge rate and depends more on the head difference between the perched aquifer and bedrock. This minimum value should approach about 1.0×10^{-4} m/day (37 mm/year) for the aquitard thickness of 20 m (the upper range of thickness for the whole area). Fig. 10d illustrates that for the cases with surface recharge of 1.2×10^{-5} and 1.2×10^{-4} m/day the critical aquitard layer thickness approaches infinity. So, in this case the water would uniformly percolate over the entire area.

5. Excess percolation rate

To make our solution more general and applicable the average surface recharge of 0.7 mm/day during mining conditions [33,37] was selected as the surface recharge and also chosen as a limit for identifying the enhanced percolation rate. With surface percolation of 0.7 mm/day, the areas with percolation rates higher than this value can act as a bioherm and collect water from surrounding parts. Accordingly, the average excess percolation rate was defined and calculated. It was determined as the difference between the value calculated with our zero order solution, within a radial distance of 170 m, and 0.7 mm/day. The excess percolation rate can be regarded as the enhanced percolation rate and shows how much the area acts as a "leaky" bioherm. The excess percolation rates were plotted for various amounts of average aquitard thicknesses and a range of head differences between the perched aquifer and

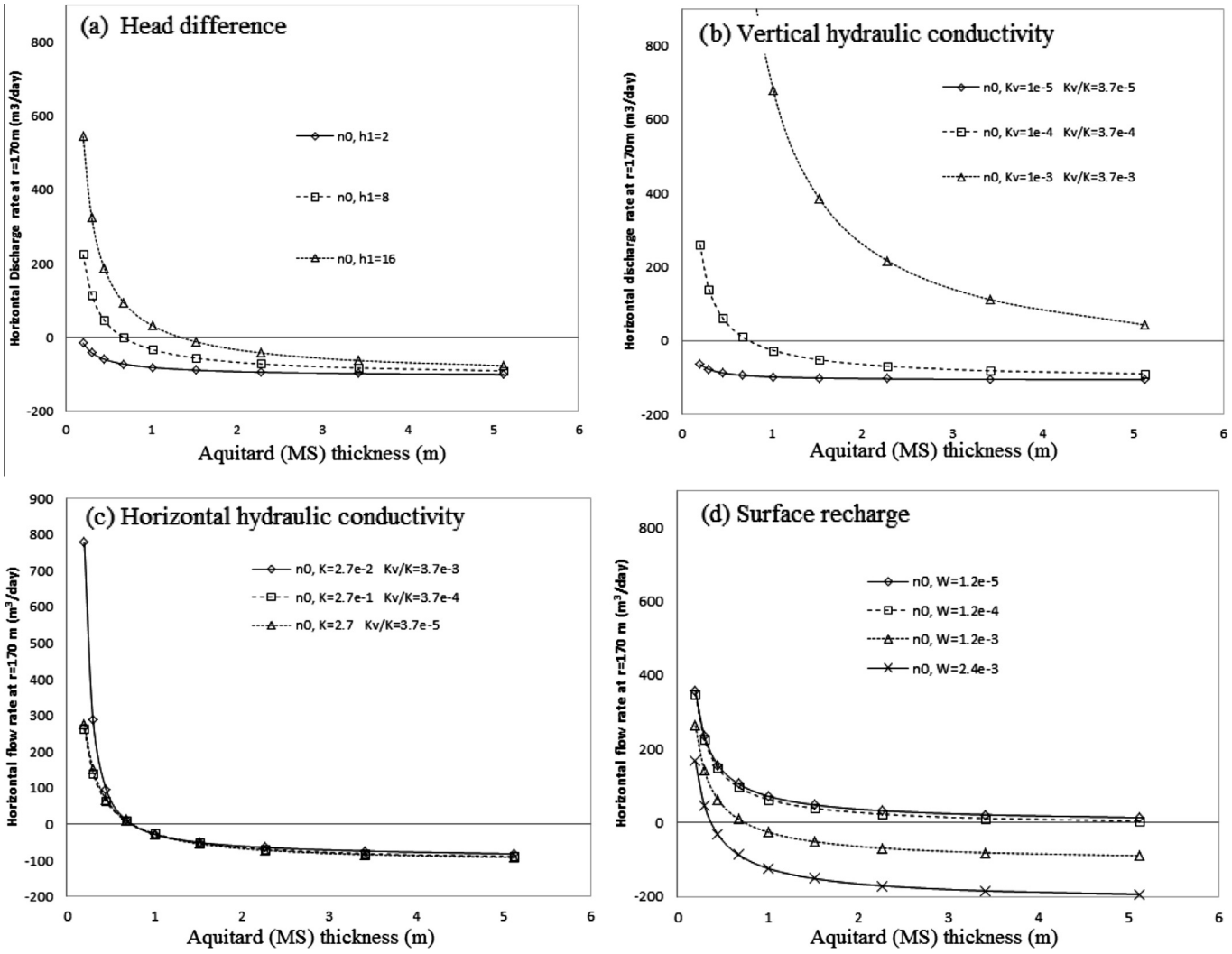

Fig. 10. Variations of horizontal discharge rate (m^3/day) versus MS layer thickness at r =170 m, for various (a) head difference (h1) values between perched aquifer and bedrock, in m, (b) vertical hydraulic conductivity in aquitard layer (K_v), in m/day, (c) horizontal hydraulic conductivity in perched aquifer (K), in m/day and (d) recharge rate from surface, W, in m/day, by the MSn0 solution.

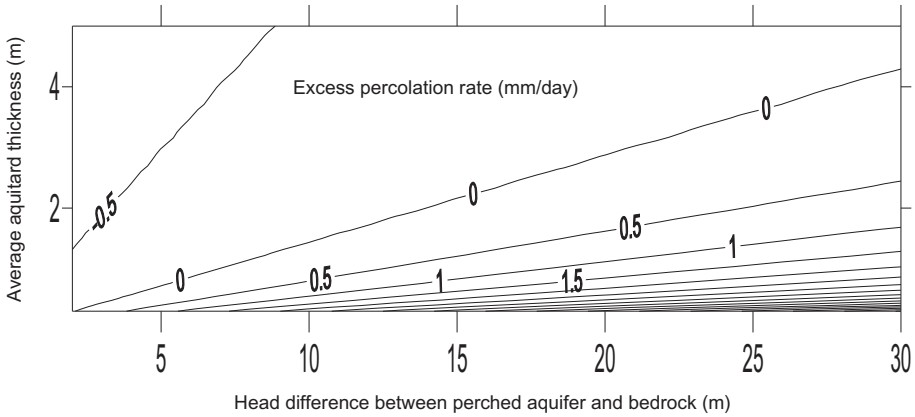

Fig. 11. Average excess percolation rate (mm/day) within radial distance of 170 m from the bioherm center for different average aquitard (MS) thickness (m) and head difference between perched aquifer and the bedrock (m).

bedrock (Fig. 11). The zero line shows the maximum aquitard thickness at which the area can act as a "leaky" bioherm for the given difference between the heads in perched aquifer and the bedrock.

6. Summary and conclusions

In this study sets of analytical solutions for the vertical downward percolation of water from the perched aquifer through the aquitard (MS) to the bedrock were developed, for different patterns of aquitard thicknesses around a bedrock (bioherm) exposure. The solutions are for saturated media and cylindrical coordinates that represent the conditions occurring in peat (perched aquifer) surrounding a bioherm, such as occur in the James Bay Lowlands. In these solutions a constant thickness perched aquifer with high permeability overlies the aquitard layer whose thickness is constant or radial-symmetrically increasing outward from the bioherm, represented by power functions of 0, 1 and 2 orders (MSn0, MSn1 and MSn2, respectively). The solutions were conducted assuming constant saturated thickness and variable piezometric head in the perched aquifer, constant recharge/discharge rate to/from the surface and that the head difference between the bottom of the saturated perched aquifer and the top of the bedrock aquifer controls the vertical flow in the aquitard layer. To generalize the solutions and make them applicable for the bioherms with different dimensions, the solutions were then transformed to their dimensionless forms and their corresponding dimensionless curves of head versus radial distances were drawn for different conditions. The field data were fitted to the dimensionless curves. The best fit was between the solution for constant aquitard thickness with order zero, MSn0, with RMS = 7.18×10^{-5} m^2 for 4 measured field values. For solutions with a higher order power function controlling aquitard thickness away from the bioherm (MSn1 and MSn2 solutions) and another approach using the Todd and Mays [35] solution, RMS of the fits were 4.17×10^{-3}, 1.27×10^{-2} and 2.32×10^{-3} m^2, respectively. Based on the better performance of the MSn0 solution, and using the measured values of $K = 0.27$ m/day [25,28], and then alternatively using either known values of $K_v (1.0 \times 10^{-4}$ m/day) to fit A_{n0}, then known (fitted) values of A_{n0} (1.2 m) to fit K_v, the best fit values were close to the measured ones; $K_v = 1.6 \times 10^{-4}$ m/day and $A_{n0} = 0.73$ m, respectively.

In our solution with constant aquitard layer thickness (MSn0), it was found that the aquitard thickness reaches a critical value in which the percolation rate from the bottom of the perched aquifer is equal to the recharge rate from its surface whereby the water in the perched aquifer is almost static because the water level is horizontal. For this study area with field head observations, measured average perched aquifer hydraulic conductivity of 0.27 m/day and measured surface recharge of 0.0012 m/day (around June 27, 2012), the critical aquitard layer thickness is about 0.7 m. For aquitard thickness less than the critical value the horizontal flow in perched aquifer is toward the bioherm (the bioherm is active) but if aquitard thickness is more than 0.7 m the flow is outward (the bioherm is inactive). The observed flow on June 27, 2012, was toward the bioherm. The critical aquitard layer thickness is the maximum thickness at which a bioherm is active and hence plays a role in collecting water from the surrounding area. The percolation rate and the horizontal flow toward the bioherm are more sensitive to aquitard thickness changes when the aquitard thickness is smaller than the critical value. For the aquitard thicknesses >20 m the percolation rate approaches to a negligibly small value.

On June 27, 2012, when conditions were relatively steady, and with surface recharge of 0.0012 m/day the average percolation rate within the radial distance of 97–170 m was calculated with the MSn0 solution as 0.00123 m/day. From this it can be concluded that the average aquitard layer thickness was less than the critical value of 0.7 m. The total net outflow from top and bottom of the perched aquifer for this area defined by the stated interval was 1.79 m^3/day, and the horizontal flow rate toward the bioherm center at a radius of 95 m was 0.49 m^3/day.

By changing the head differences between the perched aquifer and bedrock from pre-mining to current (27 June, 2012) and post-mining, with head differences of 2, 8 and 16 m, respectively, the average percolation rates would change from 5.0×10^{-4} to 1.2×10^{-3} and 2.0×10^{-3} m/day, respectively. The pre-mining value is comparable with the reported average percolation rate of 7.12×10^{-6} to 7.12×10^{-5} m/day (2.6 to 26 mm/year) for pre-mining conditions (HCI [33], Table B-8).

The results also demonstrate that for the vertical hydraulic conductivity of the aquitard layer of around 1.0×10^{-4} m/day there is a balance between the surface recharge and percolation rates; however, for vertical hydraulic conductivity of about 1.0×10^{-5} m/day, even for aquitard layer thickness approaching zero, the bioherm does not gain water from the surrounding area. When vertical hydraulic conductivity was set to 1.0×10^{-3} m/day, an extensive area around the bioherm, with aquitard layer thickness of less than about 7 m, would behave similarly to the bioherm and collect water from the outer parts. The horizontal hydraulic conductivity in perched aquifer is also an important factor in performance of a bioherm through its influence on the horizontal hydraulic gradient around it. For horizontal hydraulic conductivities smaller than about 2.7×10^{-2} m/day, the percolation rate around the bioherm is less sensitive to aquitard layer thickness around it.

Percolation rates are also sensitive to the rate of surface recharge as long as the surface recharge is more than about 1.2×10^{-4} m/day. For the surface recharge of less than 1.2×10^{-4} m/day the percolation rate approaches a minimum value of about 9.7×10^{-4} m/day for the areas close to the bioherm with aquitard layer critical thickness of 0.7 m; this minimum approaches 1.0×10^{-4} m/day (36.5 mm/year) for aquitard layer thickness of about 20 m, which is similar to the reported value for the un-impacted area. The important point is that for the aquitard layer thickness of about 20 m the percolation rate is almost independent of surface recharge.

It was found that the Todd and Mays solution, for its lack of dependency on underlying layer hydraulic conductivity, and without the limitation of keeping the flow rate zero at the center, is a valid method for comparison to the case of constant aquitard layer thickness (MSn0). The calculated average percolation rate by the Todd and Mays method in the interval between 95 and 170 m is 1.2×10^{-3} m/day and is very close to the value calculated using the MS solution with constant aquitard thickness.

In other studies [20] the vertical recharge rate for the Northern bioherm is reported in the range of 0.082–4.8 mm/day which bounds the average recharge rate of 1.23 mm/day using the MSn0 solution for June 27, 2012. Furthermore, in their study they reported vertical hydraulic conductivity of the aquitard layer as 1–10 mm/day, which is larger than our estimates of 0.10–0.16 mm/day. It is possible that the smaller vertical hydraulic conductivity suggested by the MSn0 solution reflects the existence of weathered bedrock below the aquitard layer that has a low hydraulic conductivity (our visual field observations of exposures show fractures in the upper bedrock layers are filled with marine sediments, suggesting poor transmissivity), and the calculated value is the resultant vertical hydraulic conductivity for aquitard layer and weathered bedrock. Finally, for the case of an aquitard layer with zero order, there is no water divide around the bioherm and the water divide or the capture boundary of the bioherm can be only defined from the cases with aquitard thickness of first or second order and the Todd and Mays method. By the Todd and Mays method the capture zone of the Northern bioherm for surface recharge rate of 1.2×10^{-3} m/day is 686 m.

One of the most important results here is that if the water is sufficiently available on the surface and by presuming the homogeneous aquitard layer and head difference of 8 m between the perched aquifer and bedrock, the areas with enhanced percolation rates (more than 1.2×10^{-3} m/day) are where the aquitard layer thickness is less than 0.7 m. By increasing the difference between the heads in the perched aquifer and the bedrock to 16 m, the threshold aquitard layer thickness for enhanced percolation rates increases to 1.3 m. The average percolation rate within a radial distance of 170 m from the bioherm, for average regional surface recharge of 0.7 mm/day, calculated by our zero order solution for various average aquitard thicknesses and head differences (between the perched aquifer and bedrock) were calculated. By gradually increasing the head difference between the perched aquifer and bedrock from 2 to 30 m, the minimum aquitard thickness required to constrain excess percolation through the aquitard layer changes from 0.3 to 4.3 m. For the mining industry, the message to the regulatory bodies concerned about desiccation of peatlands surrounding bioherms is that the area of potential concern is only where aquitard thickness is less than several meters, in areas of low to moderately high bedrock aquifer depressurization. The solution for the variable thickness aquitard is applicable for areas where it separates a surficial unconfined leaky aquifer and a highly permeable bedrock, particularly where local thinning of the aquitard creates radial flow toward the thinner part.

Acknowledgements

We are grateful to De Beers, especially the assistant of B. Steinback, and a the Natural Sciences and Engineering Research Council of Canada for a Collaborative Research and Development (CRD) grant awarded to J. Price and others. Thanks also for comments provided by S. Ketcheson and P. Whittington on a draft of this manuscript.

Appendix A. Radially symmetric changes in aquitard layer

In symmetric bioherms the depth of bedrock or the aquitard layer thickness is radial-symmetrically increasing outward from its center. For the sake of simplicity different trends of change in aquitard layer thickness around a bioherm were approximated by the power functions with different orders as follow:

$$t = A \times r^n \tag{A.1}$$

in which t is the aquitard thickness, n is the order of function that can be equal to 0, 1 and 2 for MSn0, MSn1 and MSn2, respectively, r is the radius from the bioherm center, and A is a coefficient showing the relation between the layer thickness and radius.

The coefficients A and its substitutes A_{n0}, A_{n1} and A_{n2} which are used in Eq. (A.1) for the Todd and Mays solution, MSn0, MSn1and MSn2 were determined by fitting the functions to the borehole data for aquitard thickness (Fig. A.1). A_{n0}, A_{n1} and A_{n2} are aquitard layer thickness, rate of change in aquitard layer thickness with radial distance and the rate of change of aquitard thickness along the radius per unit radial distance, respectively. The A_{n0}, A_{n1} and A_{n2} values determined for MSn0, MSn1 and MSn2 cases are 1.2, 6.3×10^{-3} and 3.7×10^{-5}, respectively. Fig. A.1 shows the plots of aquitard layer thickness versus radial distance from the bioherm center by Eq. (A.1) and optimum values for their corresponding A values.

Appendix B. Optimum dimensionless parameters

The optimization results for the dimensionless curves based on their best fit with the field data are illustrated in Table B.1. The data for transect 8 in June 27, 2012 were fitted to the dimensionless curves of Todd and Mays solution, MSn0, MSn1 and MSn2 and for both conditions of variable KK_{n0}, KK_{n1} and KK_{n2} and variable KK_{n0}, KK_{n1} and KK_{n2} and W_D. The optimum values for combined dimensionless variables have an infinite number of solutions for their corresponding dimensional variables. That is, when an optimum value for a dimensionless variable such as W_D is determined, it means that there are an infinite number of values for dimensional variables W and K whose ratios are equal to the optimum value of W_D, and all of these values can be an answer. Therefore, to determine the exact values for a dimensional variable, the values for the other dimensional variables should be known or assumed. For example in MSn0 by knowing h_1 = 8.97 m, r_1 = 132.57 m and assuming K = 0.27 m/day, and taking into account the optimum values for $KK_a = 4.55 \times 10^{-3}$ and $W_D = 4.45 \times 10^{-3}$ for MSn0 (Table B.1), the dimensional variables K_v/A_{n0} and W were determined as 1.37×10^{-4} day^{-1} and 1.2×10^{-3} m/day (Table B.1), respectively, based on the equations given in Table 1.

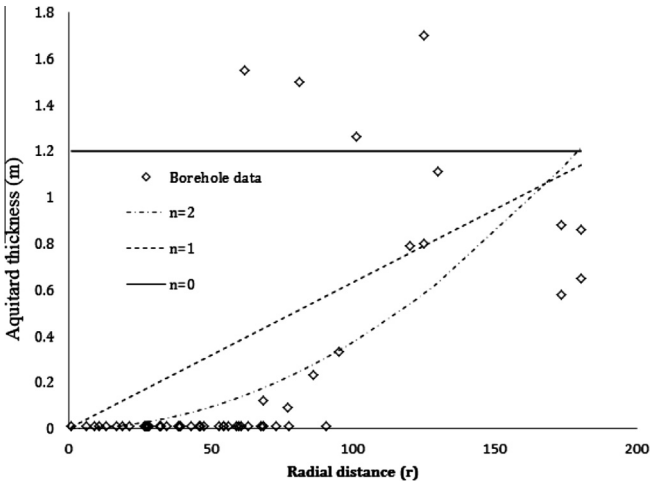

Fig. A.1. The aquitard thickness versus the radial distance from the bioherm center based on the bore hole data around Northern bioherm, beside the fitted functions with orders 0, 1, 2.

Appendix C. Determination of dimensional variables

The dimensional percolation rates from perched aquifer to bedrock were calculated by using the optimum dimensionless variables presented in Table B.1. As discussed in Appendix B the optimum values for the dimensional variables were determined by measuring or assuming the values for other variables. Here, by using the measured average value of K = 0.27 m/day, according to the field measurements presented in Whittington and Price [20], the optimum values for n, W and the ratios $K_v/A, K_v/A_{n0}, K_v/A_{n1}$ and K_v/A_{n2} were determined for different cases (Table B.1). In the Todd and Mays and MS solutions, by knowing the ratios $K_v/A, K_v/A_{n0}, K_v/A_{n1}$ and K_v/A_{n2} the percolation rate from perched aquifer to the bedrock were determined and it was not necessary to know the values of K_v, A, A_{n0}, A_{n1} and A_{n2} individually. However, to assess the values of K_v, A, A_{n0}, A_{n1} and A_{n2}, one of K_v or A (including A_{n0}, A_{n1} and A_{n2}) values should be known or presumed. Here, in the first approach, "Known K_v", the values of A_{n0}, A_{n1} and A_{n2} were determined based on the measured value of K_v, equal to 1.0×10^{-4} m/day [25,28,38]. In the second approach, "Known A_{n0}", the K_v values were calculated based on A (A_{n0}, A_{n1} and A_{n2}) values approximated by fitting functions, with corresponding orders, to the aquitard thickness data measured in the field

(Appendix A). The results of this approach for the MSn0 solution are presented in Table 3.

Appendix D. Numerical solution for MSn0

By using Hydrus 3D in a cylinder with 300 m radius and 20 m thickness, a perched aquifer on the top with 3 m thickness and hydraulic conductivity of 0.27 m/day was considered. Below the perched aquifer an aquitard layer with thickness of 0.73 m and permeability of 1.0×10^{-4} m/day was considered. A surface boundary with constant recharge of 1.2×10^{-3} m/day and a lateral constant head boundary with head of 3.86 m from the perched aquifer bottom, calculated by MSn0 method, was reserved on radial distance of 300 m. The same head difference between the perched aquifer and the bedrock layer (8.86 m), below the aquitard was set at the bedrock bottom on the model.

References

[1] Siegel D, Ericson S, Hydrology and water quality of the Copper–Nickel study region, northeastern Minnesota, U.S. Geol. Surv. Water-Resour. Investig., 80739, Minnesota; 1980.
[2] Yorath C, Kung R, Franklin R, Geoscape victoria. Geol. Surv. of Canada, Vancouver; 2002.
[3] Apple B, HW R, Summary of hydrogeologic conditions by county for the state of Michigan. U.S. Geol. Surv., Michigan; 2007.
[4] Jacob C. Radial flow in a leaky artesian aquifer. Trans Am Geophys Union 1946;27:198–208. http://dx.doi.org/10.1029/TR027i002p00198.
[5] Hantush M, Jacob C. Non-steady radial flow in an infinite leaky aquifer. Trans Am Geophys Union 1955;36:95–100. http://dx.doi.org/10.1029/TR036i001p00095.
[6] Hantush M. Modification of the theory of leaky aquifers. J Geophys Res 1960;65:3713–26. http://dx.doi.org/10.1029/JZ065i011p03713.
[7] Neuman S, Witherspoon P. Theory of flow in a confined two aquifer system. Water Resour Res 1969;5(4):803–16. http://dx.doi.org/10.1029/WR005i004p00803.
[8] Moench A, Barlow P. Aquifer response to stream-stage and recharge variations. I. Analytical step-response functions. J Hydrol 2000;230(3–4):192–210. http://dx.doi.org/10.1016/S0022-1694(00)00175-X.
[9] Butler JJ, Zhan X, Zlotnik V. Pumping-induced drawdown and stream depletion in a leaky aquifer system. Ground Water 2007;45(2):178–86. http://dx.doi.org/10.1111/j.1745-6584.2006.00272.x.
[10] Wen Z, Huang G, Zhan H. Non-Darcian flow to a well in a leaky aquifer using the Forchheimer equation. Hydrogeol J 2011;19(3):563–72. http://dx.doi.org/10.1007/s10040-011-0709-2.
[11] Freeze R, Cheery J. Groundwater. Englewood Cliffs, NJ: Prentice-Hall Inc.; 1979.
[12] Cheng A, Morohunfola O. Multilayered leaky aquifer systems: 1. Pumping well solutions. Water Resour Res 1993;29(8):2787–800. http://dx.doi.org/10.1029/93WR00768.
[13] Hunt B, Scott D. Flow to a well in a two-aquifer system. J Hydrol Eng 2007;12(2):146–55. http://dx.doi.org/10.1061/(ASCE)1084-0699(2007)12:2(146).
[14] Malama B, Kuhlman K, Barrash W. Semi-analytical solution for flow in leaky unconfined aquifer–aquitard systems. J Hydrol 2007;346(1–2):59–68. http://dx.doi.org/10.1016/j.jhydrol.2007.08.018.
[15] Malama B, Kuhlman K, Barrash W. Semi-analytical solution for flow in a leaky unconfined aquifer toward a partially penetrating pumping well. J Hydrol 2008;356(1–2):234–44. http://dx.doi.org/10.1016/j.jhydrol.2008.03.029.
[16] Hunt B. Stream depletion for streams and aquifers with finite widths. J Hydrol Eng 2008;13(2):80–9. http://dx.doi.org/10.1061/(ASCE)1084-0699(2008)13:2(80).
[17] Chen C, Jiao J. Numerical simulation of pumping tests in multiplayer wells with non-Darcian flow in the wellbore. Ground water 1999;37(3):465–74. http://dx.doi.org/10.1111/j.1745-6584.1999.tb01126.x.
[18] Cheng A. Multilayered aquifer systems: fundamentals and applications. New York: Marcel Dekker Inc; 2000.
[19] Yeh H, Chang Y. Recent advances in modeling of well hydraulics. Adv Water Resour 2013;51:27–51. http://dx.doi.org/10.1016/j.advwatres.2012.03.006.
[20] Hantush M. Flow to wells in aquifers separated by a semiprevious layer. J Geophys Res 1967;72:1709–20.
[21] Sjörs H, Bogs and Fens on Attawapiskat river, Department of Northern Affairs and National Resources, Northern Ontario; 1963.
[22] McDonald B, Glacial and interglacial stratigraphy, Hudson Bay Lowland. In: Quaternary geology of Canada and Greenland, geology of Canada, Geological Survey of Canada; 1989.
[23] AMEC, Civil geotechnical investigation, Victor diamond project feasibility study. Attawapiskat, Ontario; Geotechnical Investigation Report. Submitted to: De Beers Canada Exploration Inc., AMEC, 2003.
[24] Price J, Maloney D. Hydrology of a patterned bog-fen complex in southeastern Labrador, Canada. Nord Hydrol 1994;25:313–30. http://dx.doi.org/10.2166/nh.1994.020.
[25] Whittington P, Price J. Effect of Mine dewatering on peatlands of the James Bay Lowland: the role of bioherms. Hydrol Process 2012;26(12):1818–26. http://dx.doi.org/10.1002/hyp.9266.
[26] Cowell D. Karst Hydrogeology within a subarctic peatland: Attawapiskat River, Hudson Bay Lowland, Canada. J Hydrol 1983;61:169–75. http://dx.doi.org/10.1016/0022-1694(83)90243-3.
[27] Itasca Denver I, Dewatering of victor diamond project, March 2011 update of March 2008 groundwater flow model. Prepared for De Beers Canada, Itasca Denver Inc., Colorado; 2011.
[28] Whittington P, Price J. Effect of mine dewatering on the peatlands of the James Bay Lowland: the role of marine sediments on mitigating peatland drainage. Hydrol Process 2013;27(13):1845–53. http://dx.doi.org/10.1002/hyp.9858.
[29] Reeve A, Siegel D, Glaser P. Simulating vertical flow in large peatlands. J Hydrol 2000;227(1):207–17. http://dx.doi.org/10.1016/S0022-1694(99)00183-3.
[30] Glaser P, Hansen B, Siegel D, Reeve A, Morin P. Rates, pathways and drivers for peatland development in the Hudson Bay Lowlands, northern Ontario, Canada. J Ecol 2004;92(6):1036–53. http://dx.doi.org/10.1111/j.0022-0477.2004.00931.x.
[31] P. Whittington, The impacts of diamond mining to peatlands in the James Bay Lowlands [PhD thesis], University of Waterloo, Waterloo, Canada, 2012.
[32] HCI, Dewatering of the victor diamond mine. Predicted engineering and environmental factors, Hydrologic Consultant Inc of Colorado, Colorado; 2007.
[33] HCI, Dewatering of victor diamond project predicted engineering, cost, and environmental factors. Addendum I: update of ground-water flow model utilizing new surface-water chemistry and flow data from Nayshkootayaow river and results of sensitivity analysis, Hydrologic Consultant Inc of Colorado, Colorado; 2004.
[34] Radcliffe D, Simunek J. Soil physics with hydrus, modeling and applications. Boca Raton, London, New York: CRC Press, Taylor and Francis Group; 2010.
[35] Todd D, Mays L. Groundwater hydrology. USA: John Wiley and Sons Inc; 2005.
[36] Abramowitz M, Stegun I. Handbook of mathematical functions: with formulas, graphs, and mathematical tables, manufactured in United States of America. Courier Dover Publication; 2012.
[37] AMEC, Victor diamond project, environmental assessment comprehensive study, De Beers Canada, 2004.
[38] HCI, Dewatering of the victor diamond project. Predicted engineering, cost, and environmental factors, Hydrologic Consultant Inc of Colorado, Colorado; 2004.